Cell Proliferation

Cell Prolif., 2015, **48**, 455–464 doi: 10.1111/cpr.12198

Enhanced osteoconductivity of polyethersulphone nanofibres loaded with bioactive glass nanoparticles in *in vitro* and *in vivo* models

A. Ardeshirylajimi*,[a], S. Farhadian†,[a], F. Jamshidi Adegani‡, S. Mirzaei§, M. Soufi Zomorrod¶, L. Langroudi**, A. Doostmohammadi††, E. Seyedjafari‡‡ and M. Soleimani¶

**Department of Stem Cell Biology, Stem Cell Technology Research Center, Tehran 1997775555, Iran, †Faculty of Dentistry, Semmelweis University, Budapest 1088, Hungary, ‡Department of Molecular Biology and Genetic Engineering, Stem Cell Technology Research Center, Tehran 1997775555, Iran, §Department of Nanotechnology and Tissue Engineering, Stem Cell Technology Research Center, Tehran 1997775555, Iran, ¶Department of Hematology, Faculty of Medical Science, Tarbiat Modares University, Tehran 14115-111, Iran, **Department of Medical Immunology, Faculty of Medical Science, Tatbiat Modares University, Tehran 14115-111, Iran, ††Materials Department, Engineering Faculty, Shahrekord University, Shahrekord 8818634139, Iran and ‡‡Department of Biotechnology, College of Science, University of Tehran, Tehran 14155-6455, Iran*

Received 26 February 2015; revision accepted 3 April 2015

Abstract

Objectives: There is growing need for new scaffold constructions for synthetic bone graft substitutes to repair large bone lesions. A very promising and important class of new implants for tissue engineering is based on three-dimensional scaffolds and bioceramics.

Materials and methods: In this study, after investigation of mechanical properties of polyethersulphone (PES) nanofibres, fabricated by electrospinning methodology and coated with bioactive glass (BG), cells of the MG-63 line were cultured on surfaces of these scaffolds. Their capacity to support MG-63 proliferation was also investigated *in vitro* by MTT assay. Osteoconductivity on these scaffolds was investigated by the common osteogenic markers alkaline phosphatase (ALP) activity, calcium mineral deposition and bone-related gene activation. Next, a bone reconstruction of rat critical-size defects model was evaluated using radiographic imaging analysis (digital mammography), computed tomography and histological examination.

Results: *In vitro* results indicated that biocompatibility and osteogenic markers of MG-63 cells were significantly enhanced after coating PES with BG. Based on *in vivo* results, new bone formation in the defect site was enhanced in implanted rats in comparison with a control group. The highest reconstruction was observed in animals implanted with BG-coated nanofibres.

Conclusions: Osteoconductivity of PES nanofibres was markedly enhanced after coating them with BG, and introduction of this construct as new bone-graft substitute for bone loss and defects is indicated.

Correspondence: M. Soleimani, Faculty of Medical Science, Tarbiat Modares University, P.O. Box 14115-111, Tehran, Iran. Tel: +98 21 8886 1065 7; Fax: +98 21 8886 1065-7; E-mail: soleim_m@modares.ac.ir

[a]Both authors contributed equally this work.

Introduction

There is growing interest in a combination of bioceramics with nanofibrous scaffolds as bone implant materials (1,2). After addition of metallic and biomedical polymers, many studies have reported excellent biocompatibility and remarkable bioactivity of bioceramics (3–5). Such scaffolds are commonly used to fill bone void defects and treat bone injuries caused by accidents, trauma and more. Among these materials, bioactive glasses (BG) are one of the major ceramics used in orthopaedic surgery. BG has a network structure based on silicate or phosphate, while Na_2O and CaO play network modifier roles (6,7). Use of these materials is crucial for bone linkage and promoting new bone formation (8,9). Recently, a new technique termed 'electrospinning' has shown much promise for applicability of nanofibres in tissue engineering; it has enabled researchers to construct nanofibrous scaffolds in a versatile, relatively easy and affordable process. Nanofibres have been shown to be suitable for construction of scaffolds with high surface-to-volume ratio, and this property *via*

preparation of beneficial surfaces can affect cell adhesion, proliferation and differentiation (10–12). Nanofibres can be fabricated from different substrates, mostly polymeric materials. Polyethersulphone (PES) is a biocompatible polymer known to be an effective membrane used in haemodialysis (13–15). Recently, it has also been proven to function when electrospun into a nanofibrous scaffold that can play positive roles in *in vitro* osteogenesis (16,17).

Coating bioactive materials on scaffold surfaces is a common technique to affect their functioning, including osteoinductivity, osteoconductivity and osteogenicity. Recently, we evaluated biological behaviour of this bioceramic, and results showed that these particles enhanced viability and proliferation of bone marrow stem cells (hMSCs). In the present study, we introduced a novel approach to obtain absolute tissue engineering biomaterial, namely, BG-coated PES, for bone tissue engineering applications.

Materials and methods

Materials

Nanofibrous scaffolds fabricated by using polyethersulphone Ultrason E6020P, average molecular weight of 58 KDa, were purchased from BASF (Germany). *N*,*N*-dimethylformamide solvent and bioactive glass were purchased from Merck (Darmstadt, Germany).

In vitro *investigation*

Bioceramic coated nanofibrous scaffold preparation. In this study, an electrospinning method was used to fabricate nanofibrous PES mats. In brief, PES solution (24% wt) in *N*,*N*-dimethylformamide (DMF) after incubation at 35 °C for 4 h was drawn into four syringe pumps (5 ml) with constant mass flow rate of 0.3 ml/h. The electrospinning process was carried out using 18 kV as high voltage power supply between syringe needle and collector. Fabricated mats thickness in the order of 200 μm, were prepared over 8 h. Residual DMF evaporated using to place mats in vacuum for 24 h. BG was prepared according to protocols previously reported (18).

Then, plasma treatment was used to increase hydrophilicity of PES surfaces (pure oxygen gas, 2.45 GHz frequency; Diener Electronics, Nagold, Germany) and treated mats were punched into 1.2 cm diameter and immersed in bioactive glass/distilled water (1 mg/ml) overnight. Scaffolds were sterilized and used for subsequent surface characterization and implantation.

Characterization of electrospun nanofibres. Scanning electron microscopy (SEM, S-4500; Hitachi, Tokyo, Japan) was used for evaluation of morphology and biocompatibility of nanofibrous mats at accelerating voltage of 20 kV. Biocompatibility evaluation of nanofibres was also carried out using SEM after MG-63 cell seeding. For this reason, cell seeded-nanofibrous PES was fixed in 2.5% glutaraldehyde for 2 h (room temperature). For nanofibre dehydration, mats were passed through a series of graded alcohol concentrations, then dried.

ATR-FTIR spectroscopy and mechanical properties. FTIR-ATR analysis was used to confirm BG coating on surfaces of the nanofibrous mats using an Equinox 55 spectrometer (Bruker Optics, Ettlingen, Germany) equipped with triglycine sulphate as pyroelectric detector and diamond ATR crystal. Galdabini testing equipment was used for stability and strength investigation of the nanofibre mats. For this purpose, nanofibres were punched as 10 mm × 60 mm × 0.11 mm pieces then testing was performed at 50 mm/min crosshead speed at room temperature.

Cell seeding. After scaffold preparation and characterization, the sterilization process was performed by immersing mats in 70% ethanol for 2 h, and then immersing them in culture medium supplemented with antibiotics and anti-fungal reagent. The cells were cultured on mats at initial density of 2×10^4 per cm^2, and these were inserted into 24-well plates. After 24 h, basal medium was removed and osteogenic medium was replaced for 2 weeks. Induction medium was exchanged every 2 days.

Biocompatibility evaluation. For biocompatibility evaluation of the fabricated mats, MTT assay was performed for 5 days by culturing the MG-63 cells in three groups on tissue culture polystyrene (TCPS), PES and BG-coated PES, at 3×10^3 cells per cm^2, and incubated at 37 °C, 5% CO_2. 50 μl of MTT solution (5 mg/ml in DMEM) was added to each well containing 500 μl DMEM supplemented with 10% fetal bovine serum (FBS) every day for the 1–5 days after cell seeding.

Gene expression analysis. Relative quantification was performed, of the four most important bone gene expressions: *runt-related transcription factor 2* (*Runx2*), *collagen type 1* (*Co-1*), *osteocalcin* and *osteonectin* on MG-63 cells cultured on mats, and compared to TCPS controls at 4, 7 and 14 days. Total RNA extraction and cDNA synthesis was carried out using Revert Aid first strand cDNA synthesis kit (Fermentas, Burlington, ON,

Canada). cDNA (5 μg) was used for 40 cycles PCR in Rotor-gene Q real-time analyzer (Corbett) using Maxima SYBR Green/ROX qPCR Master Mix (Fermentas). Bone gene-related specific primers are showed in Table 1.

Alkaline phosphatase activity and calcium content assay. The alkaline phosphatase (ALP) activity assay was performed using total protein extraction of cells, cultured in all groups, by 200 ml radioimmunoprecipitation assay lysis buffer. Lysate was maintained on shakers for 20 min at 4 °C then samples were centrifuged at 14 000 ***g*** at 4 °C for 15 min; supernatant contained the total proteins. The ALP activity assay was performed using the PARS-AZMON ALP kit protocol (PARS-AZMON, Tehran, Iran). Calcium extraction was carried out for all groups using 0.6 N hydrochloric acid (Merck) followed by shaking for 2 h at 4 °C and then was also measured using to the PARS-AZMON calcium content kit protocol (PARS-AZMON).

In vivo *investigation*

Surgical procedures. In the present study, 30 male rats (Pasture Institute, Tehran, Iran) weights 300 ± 5 g, were used in the three groups (10 animals per group) control, PES implanted and BG-coated PES implanted rats. All surgical procedures were carried out in accordance with Stem Cell Technology Research Center (Tehran, Iran) guidelines. After anaesthetizing rats by intra-muscular injection of ketamine (20 mg/kg) and xylazine (2 mg/kg), cranial skin and the periosteum were raised to expose calvaria and then using a dental bur, a defect 8 mm diameter was generated in the left sides of the rat calvaria.

Radiographic and tomographic analysis. After 8 weeks implantation, after euthanizing the animals, crania of control and implanted rats were removed and placed in 10% buffered formalin. Radiographic analysis was performed using a digital mammography system (Konica Minolta, Tokyo, Japan). Spiral high-resolution medical computed tomography (CT) scanners (Siemens, Erlangen, Germany) were used for assessment of morphology of reconstructed bone at sites of the calvarial defects.

Table 1. Primers used in real-time RT-PCR

Gene	Primer sequence (F, R, 5′→3′)	Product length (bp)
HPRT1	CCTGGCGTCGTGATTAGTG TCAGTCCTGTCCATAATTAGTCC	125
Collagen-1	TGGAGCAAGAGGCGAGAG CACCAGCATCACCCTTAGC	121
Runx2	GCCTTCAAGGTGGTAGCCC CGTTACCCGCCATGACAGTA	67
Osteonectin	AGGTATCTGTGGGAGCTAATC ATTGCTGCACACCTTCTC	224
Osteocalcin	GCAAAGGTGCAGCCTTTGTG GGCTCCCAGCCATTGATACAG	80

Histological analysis. Histological evaluation was carried out on fixed samples after decalcification in natural EDTA (10%) over a week at room temperature, and dehydration in graded alcohols. Then, samples were embedded in paraffin wax, 5 μm thickness sections were cut and stained with haematoxylin and eosin (H&E), and Masson's trichrome. Samples were photographed using light microscopy (Digital Camera DXM200F; Nikon, Japan), and Image-Pro Plus software (Media Cybernetics, Bethesda, MD, USA) was used to calculate percentages of reconstructed bone.

Statistical analysis. Real-time RT-PCR data were analysed using REST 2009 software (Technical University Munich, Germany). All results are expressed as mean ± standard deviation (SD) of the mean of at least three or more independent experiments. Statistically significant differences ($P < 0.05$) between the various groups were measured using one-way analysis of variance (ANOVA). All analyses were performed using SPSS 17.0 software (SPSS, Chicago, IL, USA).

Results

Nanofibre characterization

As seen in Fig. 1a, fabricated PES scaffolds had porous structure with smooth morphology. Nanofibre diameters were between 311 and 569 nm. The contact angle of plasma-treated nanofibres was reduced to zero from 132 °C. Homogenous distribution of spherical-shaped nanoscale BG was detected along surfaces of the nanofibres in thte BG-coated PES group (Fig. 1b). PES nanofibres had tensile strength of 0.97 ± 0.1 MPa and elongation at break of 36.01 ± 2.7%, which did not significantly change after surface modification. After surface modification, it was clear that plasma treatment and BG coating had not affected scaffold properties including morphology and average diameter of nanofibres. XRD patterns of fabricated BG particles are shown in Fig. 3. Diffraction maxima observed in XRD patterns of fabricated glass after heating to 1300 °C for 10 h, indicated internal disorder and glassy nature of this material (Fig. 1c).

In addition, BG coating on surfaces of nanofibres was investigated using ATR-FTIR spectroscopy

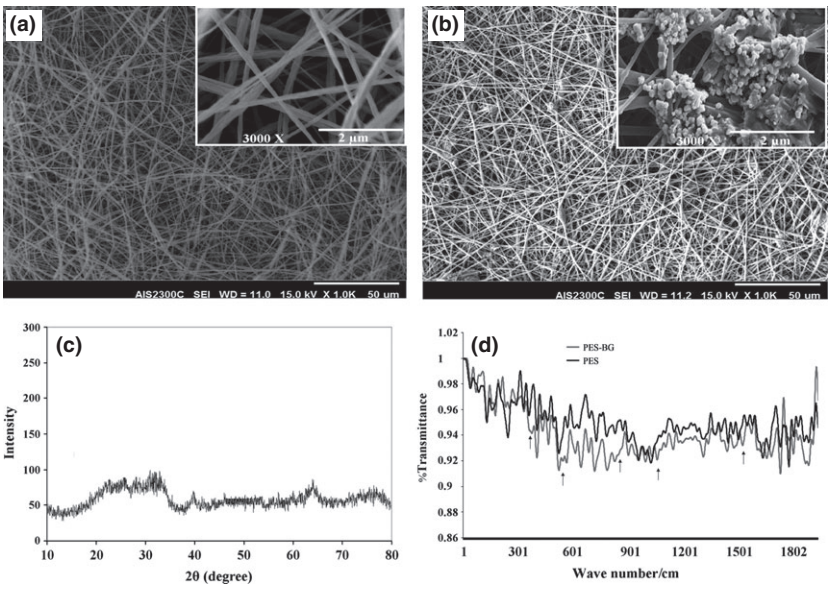

Figure 1. Morphology of polyethersulphone (PES) (a) and bioactive glass (BG)-coated PES (b) magnifications (×1000; a, b) and with higher magnification (×12 000; a, b) (insets), XRD pattern of prepared BG nanoparticles: intensity of diffraction versus angle of radiation (2θ) (c), FTIR-ATR spectra of pristine- and BG-coated PES electrospun nanofibres (d).

(Fig. 1d) before and after BG coating. After BG treatment, new peaks were developed around 400–500 cm^{-1} (Si-O-Si bend), 507 and 526 cm^{-1} (P-O Bend-Crystalline), 570 cm^{-1} (P-O Bend-Amorphous), 720–840 cm^{-1} (Si-O-Si Tetrahedral) and 1643 cm^{-1} (C-O stretch).

For biocompatibility conformation of PES nanofibres, MTT assay was used, which revealed significant viability of MG-63 cells on both types of nanofibre but with higher values for BG-coated PES compared to PES (Fig. 2).

Evaluation of osteogenic differentiation

ALP activity and mineralization. As shown in Fig. 3a, patterns of ALP activity detected in MG-63 cells cultured on PES, BG-coated PES and TCPS over the period of study were similar but their values were significantly different. From days 5–14, increasingly ALP activity was detected in cells cultured on BG-coated PES. As mineralization is a critical marker of osteogenic differentiation, calcium content assay was used for measurement of mineralization by cells cultured on TCPS, PES and BG-coated PES (Fig. 3b). Significantly highest amounts of induced mineral precipitation were observed in cells cultured on BG-coated PES in comparison to cells cultured on PES and TCPS.

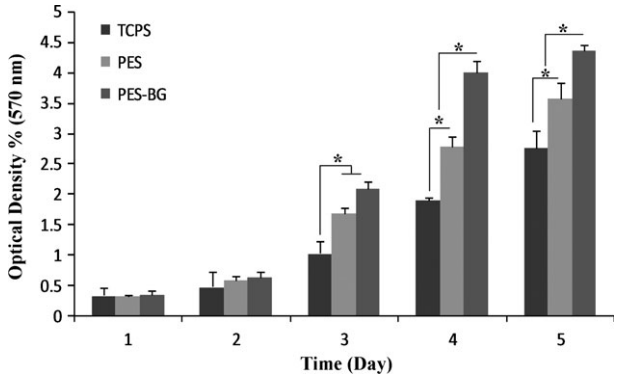

Figure 2. Viability of MG-63 cells on tissue culture polystyrene (TCPS), polyethersulphone (PES) and bioactive glass (BG)-coated PES (PES-BG) during a 1-, 2-, 3-, 4- and 5-day culture period (*indicates significant difference between the groups at $P < 0.05$).

Gene expression analysis. Results of real time RT-PCR are presented in Fig. 4. Expression of *Runx2* increased continuously in cells cultured on TCPS, PES and BG-coated PES over the 14 days. In addition, highest expression of this gene was detected at all days in the BG-coated PES group compared to the other groups. No significant change in expression of *collagen-1* was detected in any samples at day 4, but significant up-regulation was observed by day 7 in BG-coated PES compared to the other groups, and in addition at day 14, this difference was not significant between nanofibres. *Osteonectin* expression of cells cultured on BG-coated PES nanofibres at days 4 and 7 was significantly up-regulated in comparison to those cultured on TCPS and PES. At days 7 and 14, *osteonectin* expression in cells cultured on BG-coated PES was significantly up-regulated in comparison to the other groups, but on day 4, no significant difference was detected between nanofibres.

Bone reconstruction in calvarial defects

Post-surgerical macroscopic assessment. Representative macroscopic images are shown in Fig. 5. There were no sign of inflammation, local complication, wound infection, or scalp oedema at the site of implantation, after 8 weeks. All implanted nanofibres melded into the surrounding calvarial defects with no signs of encapsulation or prominent foreign body reaction. Furthermore, the nanofibres firmly held host bone tissue without any fixation (Fig. 5b). No spontaneous mineralization nor bone regenerating was observed at defect sites of control group animals at the end of study (Fig. 5c).

Evaluation of bone regeneration. Reconstructed bone at sites of calvarial defects was measured using digital mammography and multislice computed tomography (MSCT) on fixed cranial specimens at the end of the period of study. Radiological images (Fig. 6) showed that there were significant differences between animals receiving nanofibre scaffolds compared to controls ($P < 0.05$). A significant difference was also observed between animals implanted with bioceramic-coated nanofibres and uncoated nanofibres ($P < 0.05$).

Amounts of reformed bone tissue at defect sites were investigated using MSCT images of rat cranial specimens from the experimental groups (Fig. 7). In the control group, no sign of regenerated bone was observed in the animal defects (Fig. 7a). In animals that had received PES nanofibres, small amounts of bone tissue observed in defect sites (Fig. 7b). However, much more reconstruction of bone defects was detected in animals that had received BG-PES (Fig. 7c). According to results of both MSCT and digital mammography, regeneration of bone initiated from the peripheries towards centres of defect sites.

Histological findings. In addition to digital mammography and MSCT, both quality and quantity of bone reconstruction were studied using histological evaluation of defect sites of rat crania. According to H&E staining results (Fig. 8), highest amounts of bone regeneration

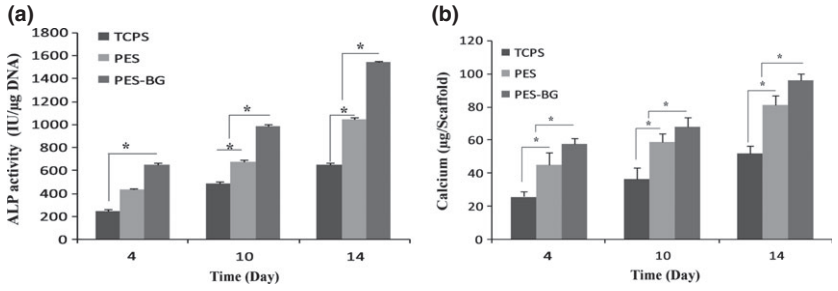

Figure 3. Alkaline phosphatase (ALP) activity of MG-63 cells on tissue culture polystyrene (TCPS), polyethersulphone (PES) and bioactive glass (BG)-coated PES (PES-BG) (a). Calcium content of stem cells on TCPS, PES and BG-coated PES (PES-BG) (b) at 4, 10 and 14 days of period of study (*indicates significant difference between the groups at $P < 0.05$).

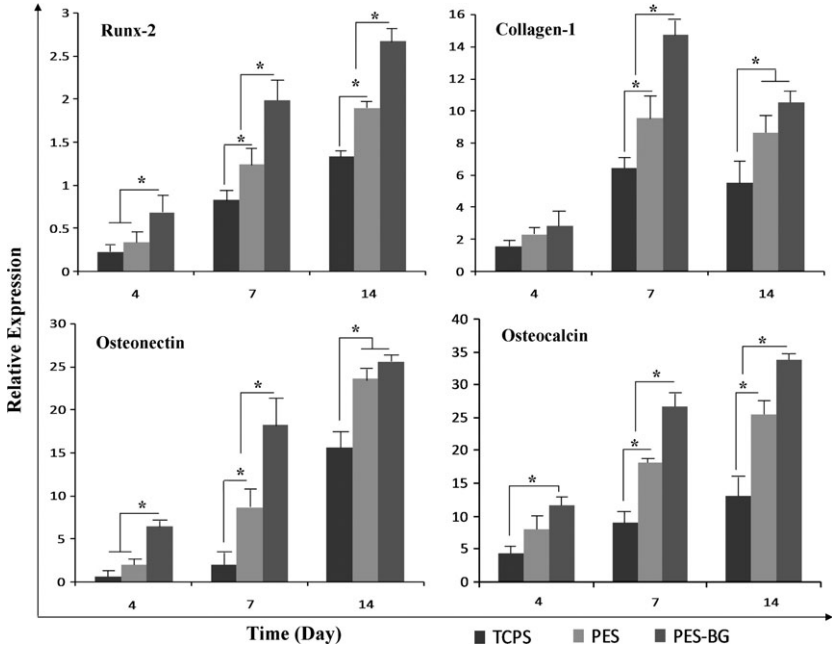

Figure 4. Relative expression of *Runx-2*, *collagen-1*, *osteonectin* and *osteocalcin* on days 4, 10 and 14 in MG-63 cells on tissue culture polystyrene (TCPS), polyethersulphone (PES) and bioactive glass (BG)-coated PES (PES-BG) of period of study (*indicates significant difference between the groups at $P < 0.05$).

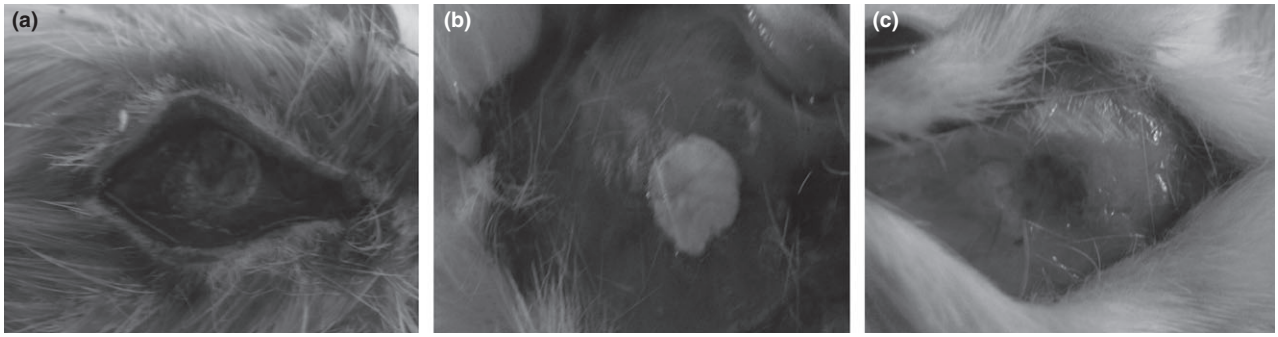

Figure 5. Critical-size defect created in rat calvaria before (a) and after 8 weeks of study with (b) or without (c) an implanted PES-BG nanofibre.

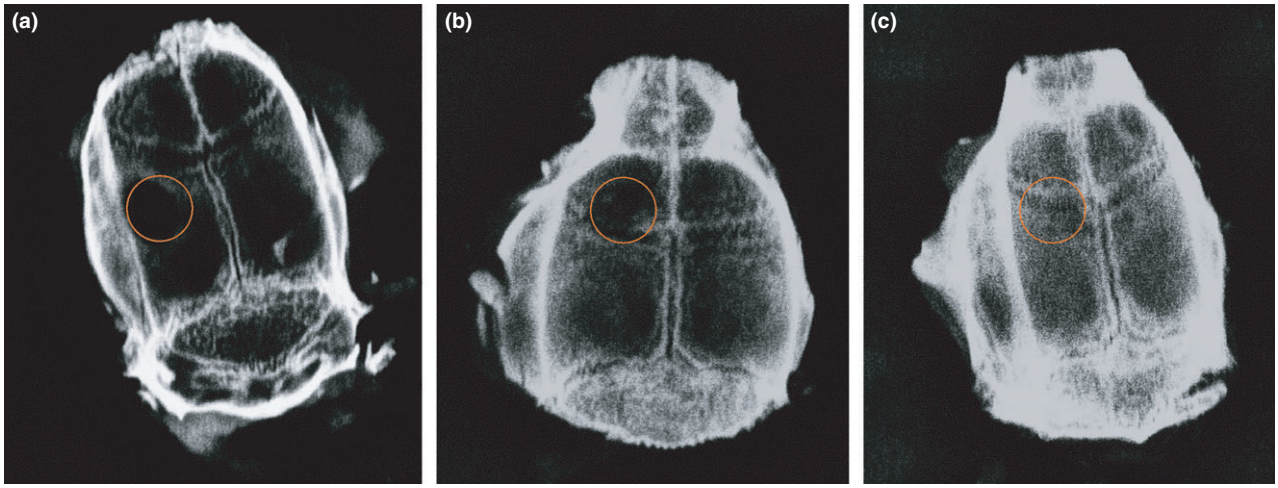

Figure 6. Digital mammography images of rat calvaria after 8 weeks study: untreated control group (a), PES (b) and BG-PES (c).

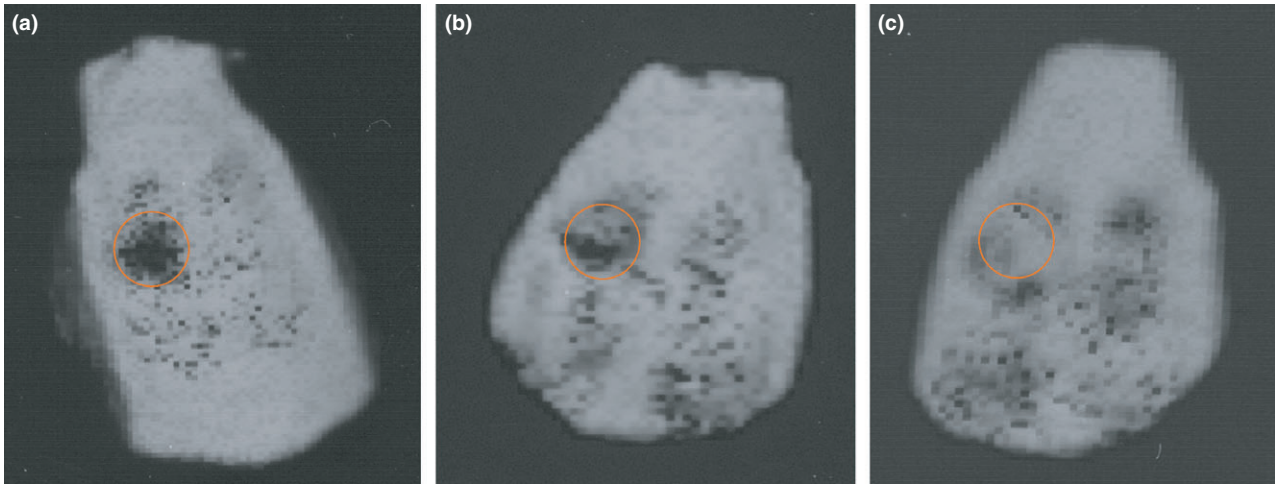

Figure 7. MSCT images of rat calvaria after 8 weeks study: untreated control group (a), PES (b) and BG-PES (c).

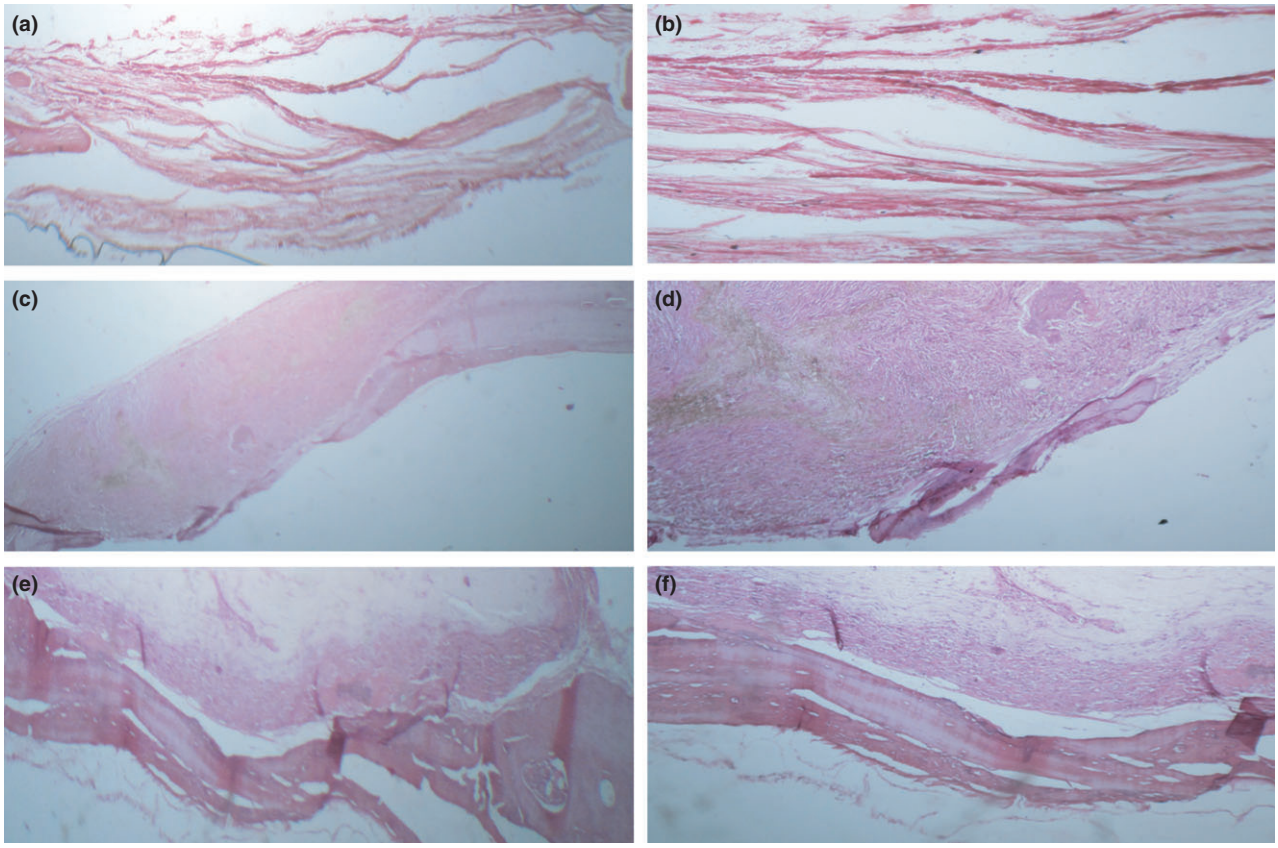

Figure 8. Optical micrographs of defects stained with H&E: untreated control group (a and b), PES (c and d) and BG-PES (e and f); two magnifications.

were observed in animals implanted with BG-PES for 8 weeks.

For analysis of collagen production by regenerated bone, Masson's trichrome staining was performed (Fig. 9). Higher levels of collagen content were detected in animals that had received BG-PES compared to PES. Areas of regenerated bone were quantified and reported as mean ± SD (Fig. 10).

Discussion

Bone graft substitutes provide important characteristics such as osteoconductivity, bioactivity and suitable mechanical properties, and so can efficiently play critical roles as accelerators in the process of bone regeneration. Of the range of different BGs introduced, bioceramics such as BG and hydroxyapatite (HA) are commonly used by orthopaedic surgeons to treat bone defects (8,19–21). However, a major drawback is their poor mechanical properties as well as brittleness which hinder their easy application and handling during implantation procedure. To overcome these problems, we proposed coating bioceramics on to surfaces of a supporting matrix which would simultaneously take advantage of bioactivity and suitable mechanical properties of the final scaffold. Recently, we tested this idea by coating HA nanoparticles on the surface of poly-L-lactide (PLLA) electrospun nanofibres and this composite showed enhancement of the osteogenic differentiation of stem cells and also induced ectopic bone formation (22). In a further study, we have also demonstrated that PES nanofibres significantly increase osteogenic differentiation of stem cells (16). In addition, we addressed bone reconstruction in animal models significantly increased when animals were implanted with PES nanofibres (17). In the present study, we have revealed that coating BG nanoparticles on surfaces of PES nanofibres lead to BGs that efficiently contributed to *in vitro* osteoconductivity and also reconstruction of calvarial bone defects in rats. Lei *et al.* have demonstrated that sol-gel-derived nanoscale BG particles enhance hydrophilicity, water absorption and degradation behaviour of PCL (23) and Moimas *et al.* fabricated bioactive glass fibrous scaffolds and studied their osteoinductivity in tibias of rabbits in comparison to 45S5 bioglass particles (24). Histological and tomographical results demonstrated that

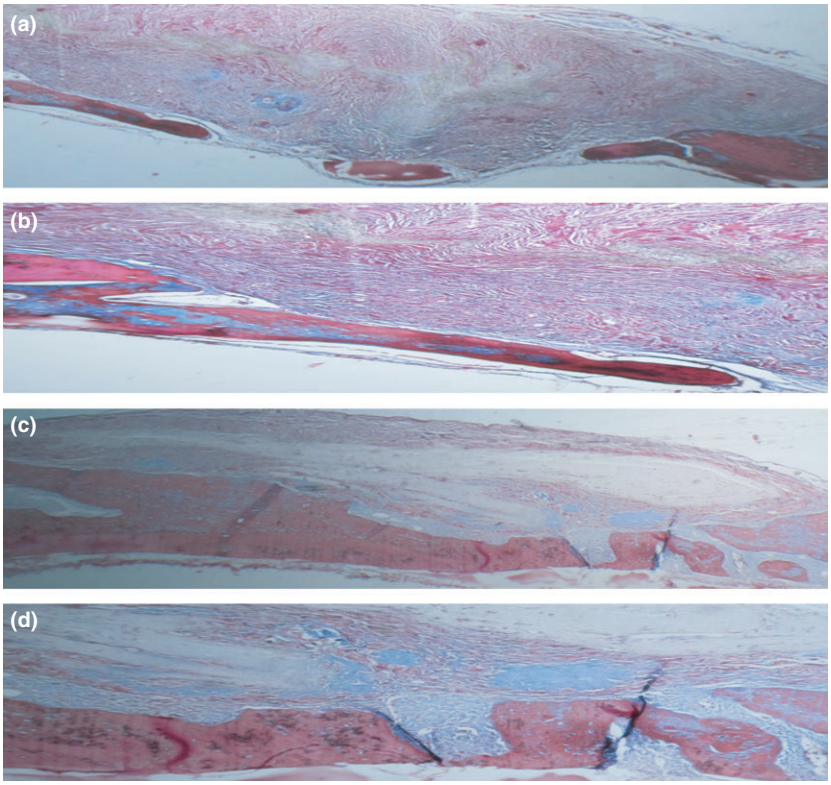

Figure 9. Optical micrographs of defects stained with Masson's trichrome: PES (a and b) and BG-PES (c and d); two magnifications.

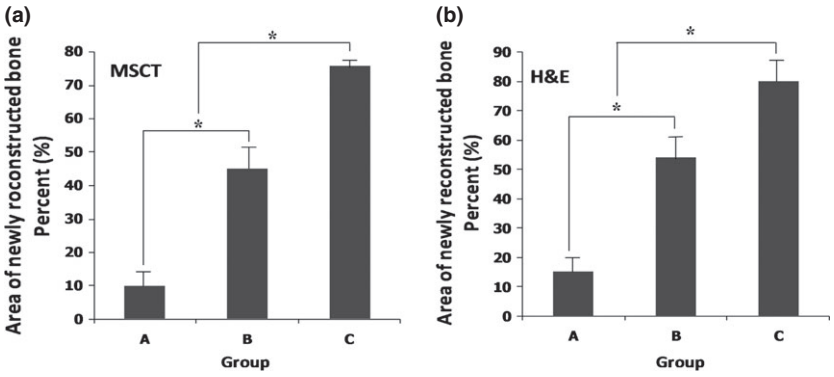

Figure 10. Area of reconstructed bone tissue resulting from quantification of MSCT (a) and H&E (b) data. Significant difference ($P < 0.05$) has been shown between the groups indicated by *. Groups specified are an untreated control group (a), PES (b) and BG-PES (c).

three-dimensional scaffold implants had greater impact on bone reconstruction and reformation compared to bioglass particles, over the period of study. In further work, Miguel *et al.* showed that SBF pre-treated scaffolds (BG fibre constructs) were more effective in rabbit calvarial bone healing compared to non-treated porous BG scaffolds, bioactive glass granules, and empty bone defects (25). Several studies have demonstrated that osteoblast proliferation, differentiation and gene expression were regulated and increased (partially) by bioactive resorbable glasses and their ionic dissolution products (26,27). Using different methods conducted in recent studies, BG particles were placed inside nanofibre constructs by electrospinning polymer/BG solutions, and biocompatibility and osteoconductivity of these fabricated composite scaffolds were evaluated (28,29). Elevated biocompatibility and osteoconductivity were observed in comparison to those of pristine nanofibres (30–32). In the same study, Noh *et al.* investigated biological behaviour of BG-coated PLLA electrospun nanofibres with a culture of osteoblasts on the surfaces of nanofibres. Improved adhesion of osteoblasts was also detected and reported (33). Neither local purulence nor inflammation was observed at sites of implantation in

any of the groups of our study. Results of histological analysis confirmed these observations and also displayed the *in vivo* biocompatibility of our nanofibrous scaffolds in the rat critical-size calvaria. In the present study, we used two quantitative methods to measure amounts of mineralization and new bone formation after implantation. Surprisingly, similar results were detected from both digital mammography and MSCT, which identified that BG-coated PES induced highest levels of bone regeneration in all groups. On the basis of the results, we showed that PES electrospun nanofibrous scaffolds coated with BG also served as osteoconductive implants. There are previous studies that have attempted to enhance bioactivity and bone-bonding strength of implants coated simultaneously with bioceramics. For instance, Yamada *et al.* displayed both biocompatibility and osteoconductivity of HA- and BG-coated titanium (34).

Finally, our results from digital mammography and MSCT were confirmed by pathology analysis reports. In addition, penetration of newly formed bone at sites of defects into the implanted scaffolds empirically demonstrated the capability of BG-coated PES nanofibrous scaffolds to induce efficient amounts of osteointegration and osteoconduction, critical for appropriate healing of orthopaedic fractures and defects.

Acknowledgements

This study was supported by Stem Cell Technology Research Center, Tehran, Iran.

References

1 Daei-Farshbaf N, Ardeshirylajimi A, Seyedjafari E, Piryaei A, Fathabady FF, Hedayati M *et al.* (2014) Bioceramic-collagen scaffolds loaded with human adipose-tissue derived stem cells for bone tissue engineering. *Mol. Biol. Rep.* **41**, 741–749.
2 Venugopal J, Prabhakaran MP, Zhang Y, Low S, Choon AT, Ramakrishna S (2010) Biomimetic hydroxyapatite-containing composite nanofibrous substrates for bone tissue engineering. *Philos.Trans. A Math. Phys. Eng. Sci.* **368**, 2065–2081.
3 Boccaccini AR, Erol M, Stark WJ, Mohn D, Hong Z, Mano JF (2010) Polymer/bioactive glass nanocomposites for biomedical applications: a review. *Compos. Sci. Technol.* **70**, 1764–1776.
4 Wang Y, Xie X, Li H, Wang X, Zhao M, Zhang E *et al.* (2011) Biodegradable CaMgZn bulk metallic glass for potential skeletal application. *Acta Biomater.* **7**, 3196–3208.
5 Bartolo P, Kruth J-P, Silva J, Levy G, Malshe A, Rajurkar K *et al.* (2012) Biomedical production of implants by additive electro-chemical and physical processes. *CIRP Ann. Manuf. Technol.* **61**, 635–655.
6 Wren A, Keenan T, Coughlan A, Laffir F, Boyd D, Towler M *et al.* (2013) Characterisation of Ga2O3–Na2O–CaO–ZnO–SiO2 bioactive glasses. *J. Mater. Sci.* **48**, 3999–4007.
7 Hill RG, Brauer DS (2011) Predicting the bioactivity of glasses using the network connectivity or split network models. *J. Non-Cryst. Solids* **357**, 3884–3887.
8 Gerhardt L-C, Boccaccini AR (2010) Bioactive glass and glass-ceramic scaffolds for bone tissue engineering. *Materials* **3**, 3867–3910.
9 Lindfors N, Hyvönen P, Nyyssönen M, Kirjavainen M, Kankare J, Gullichsen E *et al.* (2010) Bioactive glass S53P4 as bone graft substitute in treatment of osteomyelitis. *Bone* **47**, 212–218.
10 Holzwarth JM, Ma PX (2011) Biomimetic nanofibrous scaffolds for bone tissue engineering. *Biomaterials* **32**, 9622–9629.
11 Binulal N, Deepthy M, Selvamurugan N, Shalumon K, Suja S, Mony U *et al.* (2010) Role of nanofibrous poly (caprolactone) scaffolds in human mesenchymal stem cell attachment and spreading for in vitro bone tissue engineering – response to osteogenic regulators. *Tissue Eng. Part A* **16**, 393–404.
12 Dinarvand P, Hashemi SM, Seyedjafari E, Shabani I, Mohammadi-Sangcheshmeh A, Farhadian S *et al.* (2012) Function of poly (lactic-co-glycolic acid) nanofiber in reduction of adhesion bands. *J. Surg. Res.* **172**, e1–e9.
13 Barzin J, Feng C, Khulbe K, Matsuura T, Madaeni S, Mirzadeh H (2004) Characterization of polyethersulfone hemodialysis membrane by ultrafiltration and atomic force microscopy. *J. Membr. Sci.* **237**, 77–85.
14 Su B-h, Fu P, Li Q, Tao Y, Li Z, Zao H-s *et al.* (2008) Evaluation of polyethersulfone highflux hemodialysis membrane in vitro and in vivo. *J. Mater. Sci. Mater. Med.* **19**, 745–751.
15 Wang H, Yu T, Zhao C, Du Q (2009) Improvement of hydrophilicity and blood compatibility on polyethersulfone membrane by adding polyvinylpyrrolidone. *Fibers Polym.* **10**, 1–5.
16 Ardeshirylajimi A, Hosseinkhani S, Parivar K, Yaghmaie P, Soleimani M (2013) Nanofiber-based polyethersulfone scaffold and efficient differentiation of human induced pluripotent stem cells into osteoblastic lineage. *Mol. Biol. Rep.* **40**, 4287–4294.
17 Ardeshirylajimi A, Dinarvand P, Seyedjafari E, Langroudi L, Adegani FJ, Soleimani M (2013) Enhanced reconstruction of rat calvarial defects achieved by plasma-treated electrospun scaffolds and induced pluripotent stem cells. *Cell Tissue Res.* **354**, 849–860.
18 Doostmohammadi A, Monshi A, Salehi R, Fathi MH, Golniya Z, Daniels AU (2011) Bioactive glass nanoparticles with negative zeta potential. *Ceram. Int.* **37**, 2311–2316.
19 Rahaman MN, Day DE, Bal BS, Fu Q, Jung SB, Bonewald LF *et al.* (2011) Bioactive glass in tissue engineering. *Acta Biomater.* **7**, 2355–2373.
20 Jones JR, Lin S, Yue S, Lee P, Hanna JV, Smith ME *et al.* (2010) Bioactive glass scaffolds for bone regeneration and their hierarchical characterisation. *Proc. Inst. Mech. Eng. H* **224**, 1373–1387.
21 Bi L, Jung S, Day D, Neidig K, Dusevich V, Eick D *et al.* (2012) Evaluation of bone regeneration, angiogenesis, and hydroxyapatite conversion in critical-sized rat calvarial defects implanted with bioactive glass scaffolds. *J. Biomed. Mater. Res. Part A* **100**, 3267–3275.
22 Seyedjafari E, Soleimani M, Ghaemi N, Shabani I (2010) Nano-hydroxyapatite-coated electrospun poly (l-lactide) nanofibers enhance osteogenic differentiation of stem cells and induce ectopic bone formation. *Biomacromolecules* **11**, 3118–3125.
23 Lei B, Shin K-H, Noh D-Y, Jo I-H, Koh Y-H, Kim H-E *et al.* (2013) Sol-gel derived nanoscale bioactive glass (NBG) particles reinforced poly (ε-caprolactone) composites for bone tissue engineering. *Mater. Sci. Eng. C* **33**, 1102–1108.
24 Moimas L, Biasotto M, Lenarda RD, Olivo A, Schmid C (2006) Rabbit pilot study on the resorbability of three-dimensional bioactive glass fibre scaffolds. *Acta Biomater.* **2**, 191–199.
25 Miguel BS, Kriauciunas R, Tosatti S, Ehrbar M, Ghayor C, Textor M *et al.* (2010) Enhanced osteoblastic activity and bone regenera-

tion using surface-modified porous bioactive glass scaffolds. *J. Biomed. Mater. Res. Part A* **94**, 1023–1033.
26 Hoppe A, Güldal NS, Boccaccini AR (2011) A review of the biological response to ionic dissolution products from bioactive glasses and glass-ceramics. *Biomaterials* **32**, 2757–2774.
27 Hench LL (2009) Genetic design of bioactive glass. *J. Eur. Ceram. Soc.* **29**, 1257–1265.
28 Kim HW, Lee HH, Chun GS (2008) Bioactivity and osteoblast responses of novel biomedical nanocomposites of bioactive glass nanofiber filled poly (lactic acid). *J. Biomed. Mater. Res. Part A* **85**, 651–663.
29 Misra SK, Mohn D, Brunner TJ, Stark WJ, Philip SE, Roy I *et al.* (2008) Comparison of nanoscale and microscale bioactive glass on the properties of P (3HB)/Bioglass/composites. *Biomaterials* **29**, 1750–1761.
30 Zhang Y, Venugopal JR, El-Turki A, Ramakrishna S, Su B, Lim CT (2008) Electrospun biomimetic nanocomposite nanofibers of hydroxyapatite/chitosan for bone tissue engineering. *Biomaterials* **29**, 4314–4322.
31 Barakat NA, Abadir M, Sheikh FA, Kanjwal MA, Park SJ, Kim HY (2010) Polymeric nanofibers containing solid nanoparticles prepared by electrospinning and their applications. *Chem. Eng. J.* **156**, 487–495.
32 Peter M, Binulal N, Soumya S, Nair S, Furuike T, Tamura H *et al.* (2010) Nanocomposite scaffolds of bioactive glass ceramic nanoparticles disseminated chitosan matrix for tissue engineering applications. *Carbohydr. Polym.* **79**, 284–289.
33 Noh K-T, Lee H-Y, Shin U-S, Kim H-W (2010) Composite nanofiber of bioactive glass nanofiller incorporated poly (lactic acid) for bone regeneration. *Mater. Lett.* **64**, 802–805.
34 Yamada K, Imamura K, Itoh H, Iwata H, Maruno S (2001) Bone bonding behavior of the hydroxyapatite containing glass–titanium composite prepared by the Cullet method. *Biomaterials* **22**, 2207–2214.